A length-based hierarchical model of brown trout (*Salmo trutta fario*) growth and production

Jean-Baptiste Lecomte[1,2] and **Christophe Laplanche***[,1,2]

[1] Université de Toulouse; INP, UPS, EcoLab (Laboratoire Ecologie Fonctionnelle et Environnement); ENSAT, Avenue de l'Agrobiopole, 31326 Castanet Tolosan, France
[2] CNRS, EcoLab, 31326 Castanet Tolosan, France

We present a hierarchical Bayesian model (HBM) to estimate the growth parameters, production, and production over biomass ratio (P/B) of resident brown trout (*Salmo trutta fario*) populations. The data which are required to run the model are removal sampling and air temperature data which are conveniently gathered by freshwater biologists. The model is the combination of eight submodels: abundance, weight, biomass, growth, growth rate, time of emergence, water temperature, and production. Abundance is modeled as a mixture of Gaussian cohorts; cohorts centers and standard deviations are related by a von Bertalanffy growth function; time of emergence and growth rate are functions of water temperature; water temperature is predicted from air temperature; biomass, production, and P/B are subsequently computed. We illustrate the capabilities of the model by investigating the growth and production of a brown trout population (Neste d'Oueil, Pyrénées, France) by using data collected in the field from 2005 to 2010.

Keywords: Growth; Hierarchical Bayesian model; Production; Removal sampling; *Salmo trutta*.

1 Introduction

In order to evaluate, compare, and predict the status of fish populations, freshwater biologists have considered numerous descriptors of fish populations. Such variables can characterize fish stocks (Pauly and Moreau 1997; Kwak and Waters 1997; Ruiz and Laplanche 2010) duration and rates of success through life-history stages (Hutchings 2002, Klemetsen et al., 2003), phenotypic or genotypic traits (Ward, 2002; Shinn, 2010). Descriptors of fish populations can be examined separately, depending on the population aspect under focus. For instance, the impact of surface water contamination by pesticides on fish can be investigated by assessing DNA damage to blood cells (Polard et al., 2011). Aquatic resource management would rather focus on fish stock variables, such as abundance (number of fish per unit area of stream), biomass (mass of fish per unit area), production (mass of fish produced per unit area per unit time), or production over biomass ratio P/B (Pauly and Moreau, 1997). The drawback of examining a single population variable is its limited, descriptive prospect. A countermeasure would be to relate a population variable to covariates, e.g. environmental variables or descriptors of coexisting populations. As an illustration, growth of salmonids has been related to environmental factors such as temperature (Mallet et al.,

*Corresponding author: e-mail: laplanche@gmail.com, Tel: +33-534-323-973, Fax: +33-534-323-901

1999) and stream flow (Jensen and Johnsen 1999; Daufresne and Renault, 2006). Descriptors of a population can also be examined jointly. The examination of multiple variables has a more potent, explicative prospect and could improve our understanding of population dynamics (Nordwall et al. 2001).

Brown trout (*Salmo trutta*) is indigenous to Eurasia. Brown trout has been introduced to non-Eurasian freshwaters for fishing purposes. It can either grow in oceans and migrate to freshwaters for reproduction (*S. trutta trutta*), or live in lakes (*S. trutta lacustris*), or be stream-resident (*S. trutta fario*). As a result of such adaptation capabilities, brown trout has successfully colonized freshwaters to a world-wide distribution (Elliott, 1994; Klemetsen et al., 2003). Although ecologically variable, brown trout is demanding in terms of habitat and water quality. As a result, brown trout is a relevant bioindicator of the quality of freshwaters at a global scale (Lagadic et al 1998; Wood 2007). Moreover, a fundamental environmental variable driving brown trout life history is temperature (Jonsson and Jonsson, 2009), hence using brown trout as a bioindicator of climate change. Temperature affects growth (as aforementioned) as well as life-stage timing (Webb and McLay, 1996; Armstrong et al., 2003). Key life-stages of brown trout are egg laying (oviposition), hatching of larvae, emergence of fry, reproduction of adults, and death. In our case, we will focus on the effect of temperature on growth and on time between oviposition and emergence of riverine brown trout (*S. trutta fario*). We will also consider several variables characterizing stocks (abundance, biomass, production).

Abundance of riverine fish species is conveniently assessed through removal sampling: (i) a reach is spatially delimited (later referred to as a stream section), (ii) fractions of fish are successively removed of the section by electrofishing and counted, (iii) captured fish are released altogether (Lobón-Cerviá, 1991). Abundance is typically computed by using the method suggested by Carle and Strub (1978): the main statistical assumption was that the probability of capturing fish (referred to in the following as catchability) would be equal for all fish. Some contributions have shown, however, that the use of more advanced statistical models is recommendable in the aim of lowering estimation bias (Peterson et al., 2004; Riley and Fausch, 1992). The trend is to construct such statistical models within a Bayesian framework (Congdon, 2006). Recent hierarchical Bayesian models (HBMs) relate abundance to environmental covariates (Rivot et al., 2008; Ebersole et al., 2009), include heterogeneity of the catchability (Mäntyniemi et al., 2005; Do-razio et al., 2005; Ruiz and Laplanche, 2010), and can handle multiple sampling stream sections (Wyatt, 2002; Webster et al., 2008; Laplanche, 2010). The reason of popularity of HBMs over the last decade is their ability to handle complex relationships (multi-level, non-linear, mixed-effect) between variables with heterogeneous sources (relationships, data, priors) of knowledge. Freshwater biologists can statistically relate multiple descriptors of fish populations together with covariates within a single HBM framework.

We present an HBM of riverine brown trout growth and production. Our primary objective is to provide a layout to compute growth parameters of brown trout populations by using accessible data (namely removal sampling and air temperature data). Our second objective is to use such a layout to compute interval estimates of brown trout production. To fulfill the first objective, we extend the abundance model of Ruiz and Laplanche (2010) with a growth module. The abundance model performs a multimodal decomposition of length-abundance plots. Our growth module constrains parameters of the multimodal decomposition with a growth function. The interest is twofold: to guide the decomposition of length-abundance plots with a growth function and to use length-abundance plots to estimate growth parameters. Ruiz and Laplanche (2010) also created a module which computes fish biomass. To fulfill the second objective, we extend their biomass module with a production model. The overall model is the combination of eight HBMs, three (abundance, weight, biomass) related to the contribution of Ruiz and Laplanche (2010) and five to growth and production (growth, growth rate, emergence, temperature, production), which are presented successively. We show the capability of the overall model to estimate the growth parameters and the production of a brown trout population with a data set collected in the field. We discuss possible extensions of the current model.

2 Materials and methods

2.1 Notations and measured variables

A single section (of area A, m^2) of a stream populated with *S. trutta fario* is sampled by electrofishing. Electrofishing is spread over several years in a series of O campaigns with J_o removals per campaign (index over campaigns is $o \in \{1, \ldots, O\}$). The number of campaign(s) per year as well as the number of removal(s) per campaign can be variable. Time scale is daily, spans from January 1st of the year of the first campaign to December 31st of the year of the last campaign, with a total of T days. Times of campaigns are noted t_o (day). Let $C_{o,j}$ be the number of fish caught during removal $j \in \{1, \ldots, J_o\}$ at time t_o and $C_o = \sum_j C_{o,j}$ be the total number of fish caught at time t_o. The length and weight of the caught fish are measured and are noted $L_{o,j,f}$(mm) and $W_{o,j,f}$(g) ($f \in \{1, \ldots, C_{o,j}\}$). As done by Ruiz and Laplanche (2010), fish are grouped by length class: Δ_l (mm) is the length class width, I is the number of length classes, $[(i-1)\Delta_l, i\Delta_l[$ are the classes (with $[a,b[$ denoting an interval including the lower limit a and excluding the upper limit b), and $L_i = (i-1/2)\Delta_l$ are the class centers. Given class centers L_i and fish lengths $L_{o,j,f}$, the number of fish of length class i caught during removal j at time t_o can be computed and is labeled $C_{o,i,j}$ ($i \in \{1, \ldots, I\}$). The air and water temperatures on day t are noted θ_t^a and θ_t^w, respectively ($t \in \{1, \ldots, T\}$). The measured variables of the HBM are fish length and weight ($L_{o,j,f}$ and $W_{o,j,f}$), catch ($C_{o,i,j}$), stream section area (A), air and water temperatures (θ_t^a and θ_t^w). Constant (known) parameters, free (unknown) parameters of interest, and remaining (unknown) nuisance parameters are provided together in Tables 1–3, respectively.

2.2 Model structure

As briefly introduced, the overall HBM is the combination of eight submodels. Submodels are interconnected as a consequence of sharing subsets of parameters, connections between submodels

Table 1 Values of constant parameters.

Parameter	Notation	Value	Unit
Abundance			
Area	A	574.5	m^2
Length class center	L_i	–	mm
Growth			
Date of campaign	t_o	–	day
Growth rate			
Cardinal temperature	θ_{min}	3.6	°C
Cardinal temperature	θ_{max}	19.5	°C
Cardinal temperature	θ_{opt}	13.1	°C
Emergence			
Cardinal temperature	θ_0	−2.8	°C
Cardinal temperature	θ_1	22.4	°C
Date of oviposition	$t_{o,k}^{ovi}$	–	day
Critical value	CE_{50}	76.2	day

Cardinal temperatures are minimum (θ_{min}), optimum (θ_{opt}), and maximum (θ_{max}) temperatures required for growth as well as minimum (θ_0) and optimum (θ_1) temperatures required for hatching. CE_{50} is the critical value leading to the emergence of 50% of the fry. See text for values of multidimensionnal parameters ($L_i, t_o, t_{o,k}^{ovi}$).

Table 2 Distributions of free parameters (priors).

Parameter	Notation	Prior	Unit
Abundance			
Abundance	λ	Gamma(0.001,0.001)	per m^2
Cohort proportion	τ'_k	Uniform(0,1)	–
Slope	a	Normal(0,1000)	per mm
Intercept	b	Normal(0,1000)	–
Precision	$1/\sigma^2_\lambda$	Gamma(0.001,0.001)	per m^2
Precision	$1/\sigma^2_\tau$	Gamma(0.001,0.001)	–
Precision	$1/\sigma^2_a$	Gamma(0.001,0.001)	per mm
Precision	$1/\sigma^2_b$	Gamma(0.001,0.001)	–
Growth			
Optimal growth rate	G_{opt}	Lognormal(−7.25,0.30)	per day
Asymptotic length	L_∞	Lognormal(6.23,0.30)	mm
Length on $t^{\text{em}}_{1,1}$	$\bar{\mu}^0_k \vert L_\infty$	Eq. (9)	mm
Precision	$1/\sigma^2_\infty$	Gamma(0.001,0.001)	mm
Precision	$1/\sigma^2_0$	Gamma(0.001,0.001)	mm
Precision	$1/\sigma^2_\mu$	Gamma(0.001,0.001)	mm
Temperature			
Maximum water temperature	α_θ	Normal(0,1000)	°C
Inflection	β_θ	Normal(0,1000)	°C
Inflection	γ_θ	Normal(0,1000)	per °C
Minimum water temperature	μ_θ	Normal(0,1000)	°C
Precision	$1/\sigma^2_\theta$	Gamma(0.001,0.001)	°C
Weight			
Allometric	η	Gamma(0.001,0.001)	g/L
Allometric	ζ	Normal(0,1000)	–
Precision	$1/\sigma^2_\eta$	Gamma(0.001,0.001)	g/L
Precision	$1/\sigma^2_\zeta$	Gamma(0.001,0.001)	–
Precision	$1/\sigma^2_W$	Gamma(0.001,0.001)	–

Parameters are shape and rate for gamma distributions, expectation and variance for normal and lognormal distributions, and boundaries for uniform distributions. Units which are provided with precisions (e.g. $1/\sigma^2_\lambda$) are units of respective standard deviations (e.g. σ_λ). Standard deviations are related to random errors across campaigns (σ_λ, σ_τ, σ_a, σ_b, σ_η, σ_ζ), among individuals (σ_∞, σ_0), and residual (σ_μ, σ_T, σ_W).

are illustrated in Fig. 1: abundance and growth submodels depend on common parameters ($\mu_{o,k}$ and $\sigma_{o,k}$, defined later), growth depends on the time of emergence and growth rate, these quantities further depend on the water temperature, fish biomass is the cross-product of fish weight and abundance, and the combination of growth and biomass parameters lead to production. Submodels are also connected to subsets of measured variables: Fish weight ($W_{o,j,f}$) is predicted from fish length ($L_{o,j,f}$), water temperature (θ^w_t) is predicted from air temperature (θ^a_t), and abundance is related to removal sampling catch ($C_{o,i,j}$) plus stream section area (A). The model is structured into five levels : campaign ($o \in \{1,\ldots,O\}$), day ($t \in \{1,\ldots,T\}$), length class ($i \in \{1,\ldots,I\}$), removal ($j \in \{1,\ldots,J_o\}$), plus an additional level, cohort ($k \in \{1,\ldots,K\}$), which is defined later. The temperature submodel is dealt with in Appendix A (Supporting Infomation), remaining submodels are successively presented below.

Table 3 Definition of deterministic and stochastic* nodes.

Parameter	Notation	Expression	Unit
Abundance			
Population size*	$n_{o,i}$	$n_{o,i}\|\lambda_{o,i}, A \sim \text{Poisson}(\lambda_{o,i}A)$	–
Abundance	$\lambda_{o,i}$	Eq. (1)	per m^2
Weight	$\tau_{o,k}$	$\text{logit}(\tau'_{o,k})\|\tau_k, \sigma^2_\tau \sim \text{Normal}(\text{logit}(\tau_k), \sigma^2_\tau)$	–
Abundance*	λ_o	$\lambda_o\|\lambda, \sigma^2_\lambda \sim \text{Lognormal}(\lambda, \sigma^2_\lambda)$	per m^2
Abundance	$\lambda_{o,i,k}$	$\lambda_{o,i,k} = \lambda_{o,i}\,\tau_{o,k}$	per m^2
Abundance	$\lambda_{o,k}$	$\lambda_{o,k} = \lambda_o \tau_{o,k}$	per m^2
Abundance	λ_k	$\lambda_k = \lambda\tau_k$	per m^2
Population size	$n_{o,i,j}$	$n_{o,i,j} = n_{o,i,j-1} - C_{o,i,j-1}$	–
Catch*	$C_{o,i,j}$	$C_{o,i,j} \sim \text{Binomial}(n_{o,i,j}, p_{o,i})$	–
Catchability	$p_{o,i}$	$\text{logit}(p_{o,i}) = a_o L_i + b_o$	–
Slope*	a_o	$a_o\|a,\pi_a \sim \text{Normal}(a, \pi_a)$	per mm
Intercept*	b_o	$b_o\|\text{b},\pi_b \sim \text{Normal}(b, \pi_b)$	–
Growth			
Length at emergence	L_0	$L_0 = \bar{\mu}^0_1$	mm
Cohort center	$\bar{\mu}_{o,k}$	Eq. (2)	mm
Growth rate	G_t	$G_t = G_{\text{opt}} X_t$	per day
Growth rate	$\bar{G}_{o,k}$	Eq. (3)	per day
Cohort center*	$\mu_{o,k}$	Eq. (4)	mm
Cohort standard deviation	$\sigma_{o,k}$	Eq. (5)	mm
Growth rate			
Cardinal growth rate	X_t	Eq. (6)	–
Emergence			
Date of emergence	$t^{\text{em}}_{o,k}$	Eq. (7)	day
Temperature			
Expected water temperature	$\text{E}[\theta^w_t]$	Eq. (A.1)	°C
Water temperature*	θ^w_t	$\theta^w_t\|\text{E}[\theta^w_t],\sigma^2_\theta \sim \text{Normal}(\text{E}[\theta^w_t], \sigma^2_\theta)$	°C
Weight and biomass			
Weight*	$W_{o,j,f}$	$W_{o,j,f}\|\eta_o, \zeta_o, L_{o,j,f}, \sigma^2_W \sim \text{Lognormal}(\eta_o L^{\zeta_o}_{o,j,f}, \sigma^2_W)$	g
Allometric*	η_o	$\eta_o\|\eta,\sigma^2_\eta \sim \text{Normal}(\eta, \sigma^2_\eta)$	g/L
Allometric*	ζ_o	$\zeta_o\|\zeta,\sigma^2_\zeta \sim \text{Normal}(\zeta, \sigma^2_\zeta)$	–
Biomass	$B_{o,i,k}$	$B_{o,i,k} = \eta_o L^{\zeta_o}_i e^{\sigma^2_W/2} \lambda_{o,i,k}$	g/m^2
Biomass	$B_{o,k}$	$B_{o,k} = \sum_i B_{o,i,k}$	g/m^2
Biomass	B_o	$B_o = \sum_k B_{o,k}$	g/m^2
Production			
Production	$P_{o,i,k}$	Eq. (8)	g/m^2/day
Production	$P_{o,k}$	$P_{o,k} = \sum_i P_{o,i,k}$	g/m^2/day
Production	P_o	$P_o = \sum_k P_{o,k}$	g/m^2/day
Production over biomass	$(P/B)_{o,k}$	$(P/B)_{o,k} = P_{o,k}/B_{o,k}$	per day
Production over biomass	$(P/B)_o$	$(P/B)_o = P_o/B_o$	per day

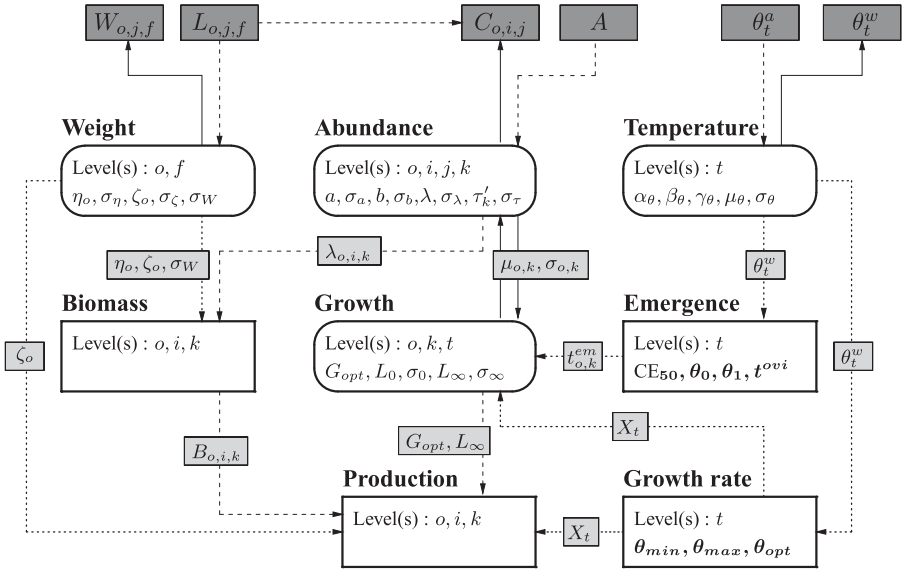

Figure 1 The overall model comprises eight submodels: Abundance, growth, growth rate, emergence, temperature, weight, biomass, and production. Large frames with rounded corners: submodels with at least one stochastic node. Large frames with right corners: submodels with deterministic nodes only. Within frames: levels, constant parameters (bold), free parameters. Light filled rectangles: variables common to pairs of submodels. Dark filled rectangles: observed variables. Full arrows: stochastic links. Dashed and dotted arrows: deterministic links. Parameters of some submodels (growth rate, emergence, temperature, weight) are precomputed and provided to parent submodels as fixed input values (dotted arrows). Remaining submodels (abundance, growth, biomass, production) form a full HBM.

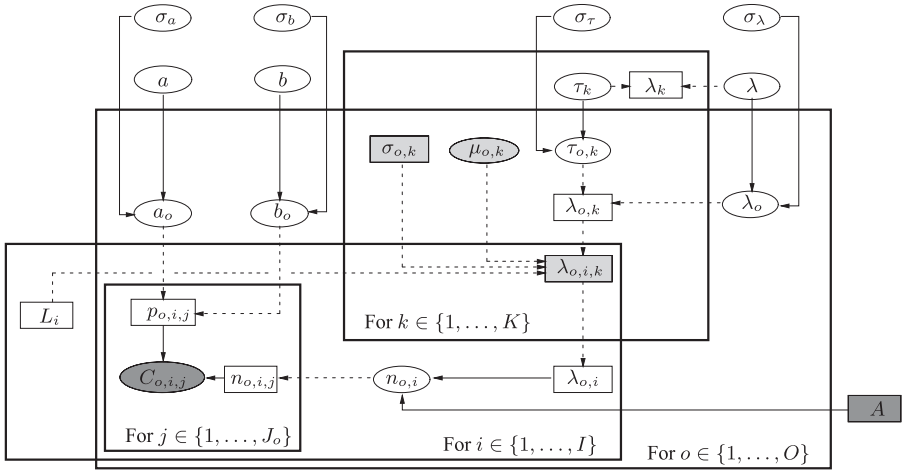

Figure 2 DAG of the abundance submodel. Frames indicate levels: campaign ($o \in \{1, \ldots, O\}$), cohort ($k \in \{1, \ldots, K\}$), length class ($i \in \{1, \ldots, I\}$), and removal ($j \in \{1, \ldots, J_o\}$). Rectangles: deterministic nodes; Ellipses: stochastic nodes; Dark filled nodes: observed variables (A, $C_{o,i,j}$); Light filled nodes: variables common to the growth ($\mu_{o,k}$, $\sigma_{o,k}$) and biomass ($\lambda_{o,i,k}$) submodels. Full arrows: stochastic links. Dashed arrows: deterministic links.

2.3 Abundance

The abundance submodel is briefly presented and is more thoroughly investigated by Ruiz and Laplanche (2010). We substitute the spatial level (stream section) presented by Ruiz and Laplanche (2010) by a time level (campaign, $o \in \{1, \ldots, O\}$). An illustration of the submodel is provided as a Directed Acyclic Graph (DAG, Fig. 2). The number of fish of length class i present in the stream section at time t_o are taken to be independent Poisson random variables, $n_{o,i}|\lambda_{o,i}, A \sim \text{Poisson}(\lambda_{o,i}A)$, where $\lambda_{o,i}$ is the expected density per unit area of fish of length class i at time t_o. The latter quantity is referred to in the following as abundance (of fish of length class i at time t_o). We define additional abundance variables at higher levels: abundance λ_o of fish (of all sizes) present in the stream section at time t_o (four more abundance variables at distinct levels are defined later). Abundance $\lambda_{o,i}$ is given by decomposing the total abundance λ_o into length classes by using a mixture of Gaussian probability density functions

$$\lambda_{o,i} = \lambda_o \Delta_l \sum_{k=1}^{K} \frac{\tau_{o,k}}{\sigma_{o,k}} F\left(\frac{L_i - \mu_{o,k}}{\sigma_{o,k}}\right), \tag{1}$$

where K is the number of Gaussian components, $\mu_{o,k}$, $\sigma_{o,k}$, and $\tau_{o,k}$ are component centers, standard deviations, and weights ($\sum_{k=1}^{K} \tau_{o,k} = 1$), respectively. An illustration of the mixture is provided in Fig. 3. We only consider the Gaussian kernel $F(l) = \exp(l^2/2)/\sqrt{2\pi}$ for the reasons provided in Appendix B (Supporting Infomation). Gaussian component indexed by o,k exclusively includes the fish born $k-1$ years before the year of campaign o, as a result components are referred to in the following as cohorts (Pitcher, 2002). Conditional distributions of cohort centers and standard deviations ($\mu_{o,k}$ and $\sigma_{o,k}$) are provided by the growth submodel. Weight $\tau_{o,k}$ of cohort k at time t_o and abundance λ_o at time t_o are variable across campaigns, $\text{logit}(\tau'_{o,k})|\tau_k, \sigma^2_\tau \sim \text{Normal}(\text{logit}(\tau_k), \sigma^2_\tau)$ and $\lambda_o|\lambda, \sigma^2_\lambda \sim \text{Lognormal}(\lambda, \sigma^2_\lambda)$, with $\tau_{o,k} = \tau'_{o,k} / \sum_{k'=1}^{K} \tau'_{o,k'}$. We partition abundance variables ($\lambda_{o,i}$, λ_o, and λ) into cohorts ($\lambda_{o,i,k}$, $\lambda_{o,k}$, and λ_k, respectively, see Table 3 and Fig. 3). The number of fish of length class i remaining in the stream section before removal j at time t_o is noted $n_{o,i,j}$, with $n_{o,i,1} = n_{o,i}$ and $n_{o,i,j} = n_{o,i,j-1} - C_{o,i,j-1}$ for subsequent removals ($j \in \{2, \ldots, K\}$). The number of fish of length class i caught during removal j at time t_o is a binomial, $C_{o,i,j} \sim \text{Binomial}(n_{o,i,j}, p_{o,i})$. The catchability is provided by a mixed-effect logit regression model $\text{logit}(p_{o,i}) = a_o L_i + b_o$ with random variability of the slope and the intercept across campaigns (Table 3). Positive (negative) value $a_o > 0$ ($a_o < 0$) indicates an increase (decrease) of the catchability with fish length. Null value $a_o = 0$ corresponds to a catchability constant with fish length, of value $p_{o,i} = \text{logit}^{-1}(b_o)$.

2.4 Growth

The growth submodel constrains cohort centers and standard deviations ($\mu_{o,k}$ and $\sigma_{o,k}$) to a growth function. We model individual fish growth by using a von Bertalanffy growth function (VBGF). We relate individual VBGF parameters to cohort VBGF parameters through a statistical model which is detailed in Appendix B (Supporting Infomation). An illustration of the growth submodel is provided as a DAG (Fig. 5, Supporting Infomation). Expected center of cohort k at time t_o is (Appendix B, Supporting Infomation)

$$\bar{\mu}_{o,k} = L_\infty - (L_\infty - L_0) \exp[-\bar{G}_{o,k}(t_o - t^{\text{em}}_{o,k})], \tag{2}$$

where $t^{\text{em}}_{o,k}$ is the date of emergence of cohort k, L_0 is the expectation (over individuals) of the length at emergence, L_∞ is the expectation (over individuals) of the asymptotic length, and $\bar{G}_{o,k}$ is the average (between $t^{\text{em}}_{o,k}$ and t_o) of the expectation (over individuals) of the daily growth rate

$$\bar{G}_{o,k} = \sum_{t=t^{\text{em}}_{o,k}+1}^{t_o} G_t / (t_o - t^{\text{em}}_{o,k}). \tag{3}$$

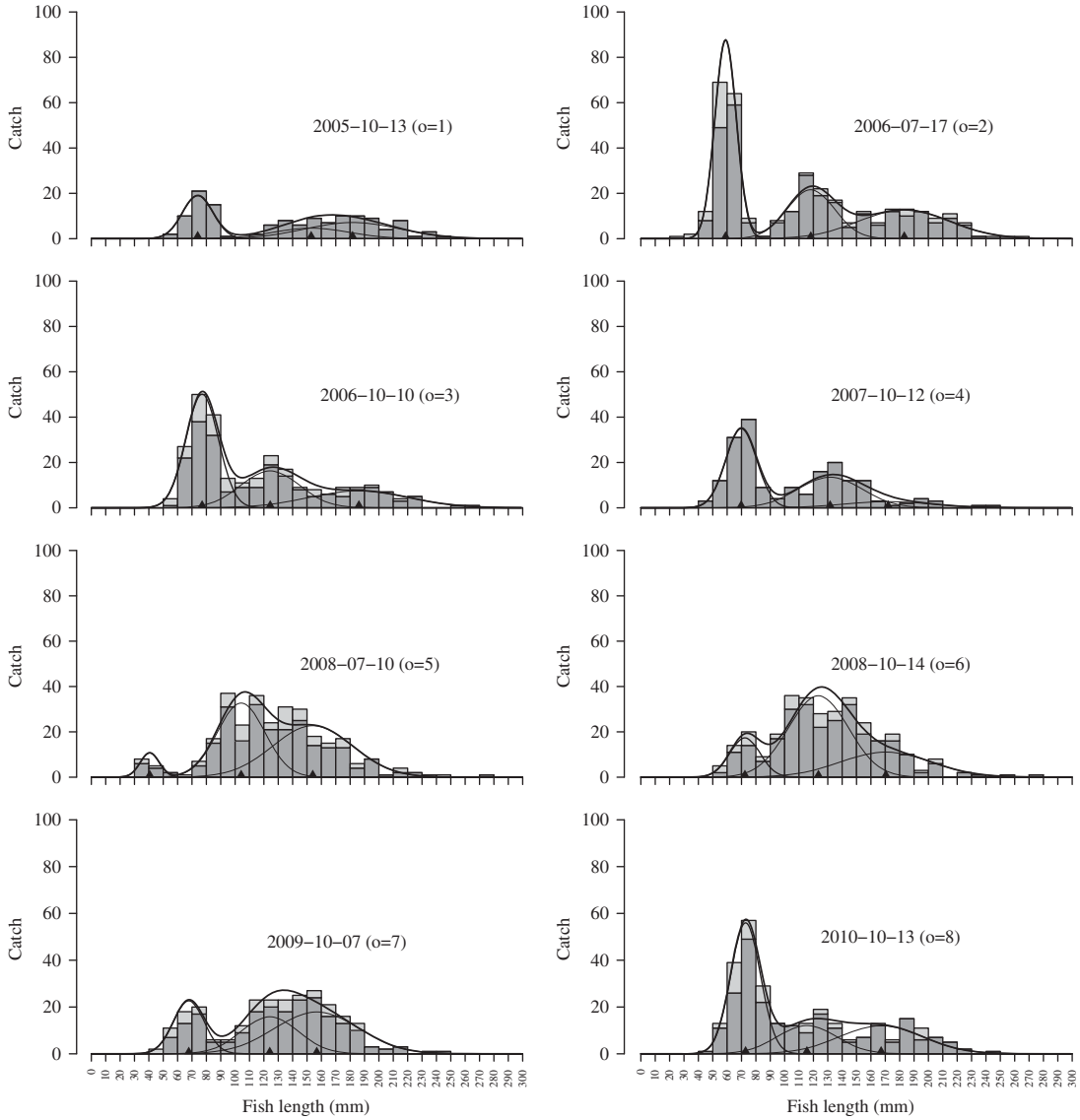

Figure 3 Number of caught fish $C_{o,i,j}$ per $\Delta_l = 10$ mm length class at Saint-Paul from October 2005 ($o = 1$) to October 2010 ($o = 8$). The number $C_{o,i,j}$ of fish of length class i caught during removal j during campaign o is illustrated as the j-th stacked sub-bar making up the bar of i-th length class (x-axis) of the subplot related to campaign o. Cohort centers ($\mu_{o,k}$, triangles) are represented. Expected population sizes per cohort ($\lambda_{o,i,k}A\Delta_l$, thin solid lines) and total ($\lambda_{o,i}A\Delta_l$, thick solid lines) are computed by using Eq. (1) with point parameter estimates of $\mu_{o,k}$, $\sigma_{o,k}$, $\tau_{o,k}$, and λ_o.

The daily growth rate G_t as well as the date of emergence $t^{\mathrm{em}}_{o,k}$ are functions of water temperature. Their expressions are provided by the growth rate and emergence submodels, respectively. We tolerate discrepancies between cohort centers $\bar{\mu}_{o,k}$ expected by the growth submodel and cohort centers $\mu_{o,k}$ used by the abundance submodel. They are equal modulo

a logit-transformed residual normal error

$$\text{logit}\left(\frac{\mu_{o,k}-\bar{\mu}^0_{o,k}}{\bar{\mu}^1_{o,k}-\bar{\mu}^0_{o,k}}\right)|\bar{\mu}_{o,k},\bar{\mu}^0_{o,k},\bar{\mu}^1_{o,k},\sigma^2_{\mu}\sim\text{Normal}\left(\text{logit}\left(\frac{\bar{\mu}_{o,k}-\bar{\mu}^0_{o,k}}{\bar{\mu}^1_{o,k}-\bar{\mu}^0_{o,k}}\right),\sigma^2_{\mu}\right), \tag{4}$$

of variance σ^2_{μ}, where $\bar{\mu}^0_{o,k}$ is the center of cohort k at the date of emergence of the year of campaign o ($t^{\text{em}}_{o,1}$) and $\bar{\mu}^1_{o,k}$ is the center of cohort k at the end of the year of campaign o (December 31th). The motivation to include this additional error term in the model is illustrated and discussed later. Variables $\bar{\mu}^0_{o,k}$ and $\bar{\mu}^1_{o,k}$ are computed with a formula similar to Eq. (2). The scaled logit transformation of Eq. (4) ensures that both $\bar{\mu}_{o,k}$ and $\mu_{o,k}$ are greater than $\bar{\mu}^0_{o,k}$ and lesser than $\bar{\mu}^1_{o,k}$. The standard deviation $\sigma_{o,k}$ is provided by

$$\sigma^2_{o,k}=\sigma^2_0\frac{[L_\infty-\bar{\mu}_{o,k}]^2}{[L_\infty-L_0]^2}+\sigma^2_\infty\frac{[\bar{\mu}_{o,k}-L_0]^2}{[L_\infty-L_0]^2}, \tag{5}$$

where σ_0 and σ_∞ are the standard deviations representative of variability among individuals of the length at emergence and of the asymptotic length, respectively (Appendix B, Supporting Infomation). We do not model growth of fish born before the year of the first campaign. The resulting edge effects are dealt with by simulating growth by starting on the date of emergence on the year of the first campaign ($t^{\text{em}}_{1,1}$). Cohort centers on such a date are labeled $\bar{\mu}^0_k$.

2.5 Growth rate and emergence

2.5.1 Growth rate

Water temperature affects fish growth (Jonsson and Jonsson, 2009). Therefore, various authors have included seasonal variability in the VBGF parameters to consider the effects of water temperature on growth (Taylor, 1960; Somers, 1988; Mallet et al., 1999). Fontoura and Agostinho (1996) have successfully modeled the growth of two freshwater fish species by using the VBGF with a growth rate as a deterministic function of water temperature. The latter authors have suggested the use of a bell-shaped relationship between temperature and growth rate, with a null growth rate below a minimum temperature (θ_{min}) or above a maximum temperature (θ_{max}) and a maximum growth rate at an optimum temperature (θ_{opt}). Mallet et al. (1999) have suggested a similar relationship to predict fish growth rate from water temperature. The latter relationship originates from the work of Rosso et al. (1995) dealing with bacterial growth with pH. We use the relationship provided by Mallet et al. (1999) to relate daily growth rate to water temperature. The daily growth rate is $G_t = G_{\text{opt}}X_t$ where G_{opt} is the growth rate at optimum temperature θ_{opt} and X_t is the cardinal daily growth rate

$$X_t=\frac{(\theta^w_t-\theta_{\text{min}})(\theta^w_t-\theta_{\text{max}})}{(\theta^w_t-\theta_{\text{min}})(\theta^w_t-\theta_{\text{max}})-(\theta^w_t-\theta_{\text{opt}})^2}, \tag{6}$$

where θ^w_t is the water temperature at time t.

2.5.2 Emergence

Water temperature affects life-stage timing of fish (Jonsson and Jonsson, 2009). Time from oviposition to hatching and time from hatching to emergence are related to water temperature (Webb and McLay, 1996; Armstrong et al., 2003). Elliott and Hurley (1998) have shown that the delay between oviposition t^{ovi} and the median date of emergence t^{em} (date when half fry have emerged) of brown trout can be well-predicted by finding t^{em} leading to $\int_{t^{\text{ovi}}}^{t^{\text{em}}}(\theta^w(t)-\theta_0)/[\theta_1-\theta^w(t)]\text{d}t=\text{CE}_{50}$, where $\theta^w(t)$ is water temperature at time t, θ_0 is the minimum temperature required for hatching, θ_1 is the optimum temperature for hatching, and CE_{50} is the critical value leading to the emergence of 50% of the fry. By approximating the latter integral by the midpoint rule with a daily time step, the

date of emergence $t_{o,k}^{\mathrm{em}}$ of fish which are present under the form of cohort k at time t_o leads to

$$\sum_{t=t_{o,k}^{\mathrm{ovi}}}^{t_{o,k}^{\mathrm{em}}} \frac{\theta_t^w - \theta_0}{\theta_1 - \theta_t^w} \simeq \mathrm{CE}_{50}. \tag{7}$$

2.6 Weight

Length and weight of fish $f \in \{1, \ldots, C_{o,j}\}$ caught during removal j at time t_o are related by the allometric formula $W_{o,j,f} = \eta_o L_{o,j,f}^{\zeta_o} \exp(\varepsilon_{o,j,f})$ with an i.i.d lognormal residual error of variance σ_W^2, $\varepsilon_{o,j,f} | \sigma_W^2 \sim \mathrm{Normal}(0, \sigma_W^2)$. Allometric parameters η_o and ζ_o are allowed to vary between campaigns and are taken independent (Table 3). Log-transformed, the latter submodel is a two-level linear mixed-effect model with a normal, heteroscedastic residual error (Pinheiro and Bates, 2000).

2.7 Model outputs: Biomass and production

The biomass of fish of length class i of cohort k at time t_o is approximately $B_{o,i,k} \simeq \eta_o L_i^{\zeta_o} e^{\sigma_W^2/2} \lambda_{o,i,k}$ (Ruiz and Laplanche 2010). The biomass of fish of cohort k at time t_o is $B_{o,k} = \sum_i B_{o,i,k}$ and the overall biomass at time t_o is $B_o = \sum_k B_{o,k}$. The production of fish of length class i of cohort k at time t_o is

$$P_{o,i,k} = \frac{\mathrm{d}B_{o,i,k}}{\mathrm{d}t} = \zeta_o \frac{B_{o,i,k}}{L_i} \frac{\mathrm{d}L_i}{\mathrm{d}t} = \zeta_o B_{o,i,k} G_o \frac{L_\infty - L_i}{L_i}, \tag{8}$$

where $G_o = G_t$ for $t = t_o$. The production of fish of cohort k at time t_o is $P_{o,k} = \mathrm{d}B_{o,k}/\mathrm{d}t = \sum_i P_{o,i,k}$ and the overall production at time t_o is $P_o = \mathrm{d}B_o/\mathrm{d}t = \sum_k P_{o,k}$. Respective production over biomass ratios are $(P/B)_{o,k} = P_{o,k}/B_{o,k}$ and $(P/B)_o = P_o/B_o$.

2.8 Constant parameters, data sets, and priors

2.8.1 Constant parameters

We use cardinal temperatures ($\theta_{\min}$, $\theta_{\max}$, θ_{opt}) suggested by Elliott et al. (1995) for *S. trutta fario*. Dates of emergence are computed from Eq. (7) by using parameter values (θ_0, θ_1, CE_{50}) provided by Elliott and Hurley (1998) for *S. trutta*. Oviposition dates are assumed equal for all years (October 20th). Values of constant parameters are provided in Table 1 and are highlighted in Fig. 1.

2.8.2 Data sets

We use the model to study growth and production of resident brown trout (*S. trutta fario*) populating the Neste d'Oueil stream (Haute Garonne, Pyrénées, France). Neste d'Oueil brown trouts are the dominant species of the stream (Gouraud et al., 2001). Trouts which are considered in this case study were electrofished at a single stream section (Saint-Paul d'Oueil) $O = 8$ times from 2005 to 2010, 6 times in October (13th, 10th, 12th, 14th, 7th, and 13th from 2005 to 2010, respectively) plus twice in July (2006 July 17th, 2008 July 10th). The Saint-Paul d'Oueil stream section is 121 m long, 4.7 m wide with a 1050 m elevation. The stream section is not delimited with physical barriers, neither across removals nor across campaigns, as discussed later. Captured fish are released at the end of each electrofishing campaign. The number of fish caught $C_{o,i,j}$ is illustrated by length-abundance plots (Fig. 3). A total of 2078 fish were captured among which 875 were weighted. A description of air and water temperature data sets is provided as Supporting Infomation.

2.8.3 Priors

Growth rate G_{opt} and asymptotic length L_∞ are assigned informative independent lognormal priors. Such a choice is based on 41 estimates of growth rate and respective asymptotic length of brown trout from the literature (Froese and Pauly, 2010). Shapiro–Wilk test for multinormality shows that log-transformed growth rate and asymptotic length reasonably follow a bivariate normal distribution ($p = 0.046$). Correlation between log-transformed growth rate and asymptotic length is not significant, however ($p = 0.085$). Growth rates and asymptotic length are therefore assigned independent lognormal priors which hyperparameters are computed by using the database cited above. We set $L_0 = \bar{\mu}_1^0$. In order to fulfill the constraint $0 < \bar{\mu}_1^0 < \cdots < \bar{\mu}_K^0 < L_\infty$, we simulate independent $q_{k'} \sim \text{Uniform}(0, 1)$ ($k' \in \{1, \ldots, K+1\}$) and use the prior ($\bar{\mu}_0^0 = 0$)

$$\bar{\mu}_k^0 = \bar{\mu}_{k-1}^0 + L_\infty q_k \Big/ \sum_{k'=1}^{K+1} q_{k'}. \tag{9}$$

Remaining parameters are assigned vague priors (Table 2).

2.9 Computations

2.9.1 Precomputations

The computation resources which are required to carry out a joint simulation of the 8 submodels for 6 years are prohibitive. Fish weight, water temperature, time of emergence, and growth rate are precomputed and provided to parent models as fixed input values. This issue is discussed later. Parameters of the weight submodel are estimated by using collected fish lengths and weights. Parameters of the temperature submodel are estimated by using collected air–water temperatures (from March 2006 to October 2009). The sum of Eq. (7) is precomputed step by step by increasing the date of emergence starting on January 1st until the critical value CE_{50} is reached. The quantity $\bar{X}_{o,k} = \sum_{t=t_{o,k}^{\text{em}}+1}^{t_o} X_t/(t_o - t_{o,k}^{\text{em}})$ appearing in Eq. (3) is also precomputed. Precomputed time of emergence $t_{o,k}^{\text{em}}$ and $\bar{X}_{o,k}$ are then provided as inputs to the growth submodel.

2.9.2 BUGS simulations

Submodels, to the exception of the emergence submodel which is executed with `R` (Crawley, 2007), are implemented by using `OpenBUGS`, open source version of `WinBUGS` (Lunn et al., 2009; Ntzoufras, 2009). We simulate posterior samples of model parameters by using a Markov chain Monte Carlo (MCMC) method (Robert and Casella, 2004). Samples are processed by using `R` (Crawley, 2007). `WinBUGS` and `R` scripts as well as data files are gathered within a GPLv3 piece of software, Hierarchical Modeling of Salmonid Populations (`HMSPop`) version 2.0 (`http://modtox.myftp.org/software/hmspop`). Reported point estimates of the parameters are posterior expectation estimates. Interval estimates are 2.5 and 97.5% quantile estimates of marginal posteriors. Convergence was investigated by using the ANOVA-type diagnosis described by Gelman and Rubin (1992) with three chains. Independent samples were obtained by thinning guided through the examination of the autocorrelation functions of the posterior samples. Five hundred independent posterior samples were generated for each model. Alternative growth submodels are compared in terms of goodness-of-fit ($\bar{D}$, posterior expectation of the deviance statistics). Penalization with complexity was not feasible: it was not possible to compute complexity (effective number of parameters) as presented by Spiegelhalter et al. (2002) due to the use of a discrete node in our model ($C_{o,i,j}$), alternative estimate relying on asymptotic distribution of the deviance statistics (Gelman, 2003) did not lead to reliable results, and a manual count of stochastic parameters clearly overestimated complexity.

2.9.3 Model comparisons

In the aim of providing the most parsimonious model, we evaluate the relevance of including the emergence, temperature, and growth submodels to compute production. For that purpose, several model alternatives are compared (Table 4). The first alternative ($\mathcal{M}_1$, baseline) is the overall model which has just been presented. The second alternative ($\mathcal{M}_2$) considers that time of emergence is not temperature-dependent (April 1st for all years). The third alternative ($\mathcal{M}_3$) considers that time of emergence and growth rate are not temperature-dependent ($X_t = 1$ for all t). In that case, the growth rate at optimum temperature is equal to the growth rate averaged over the study period ($\bar{G} = G_{\text{opt}} \sum_t X_t / T$). In the aim of comparing growth rates of models $\mathcal{M}_{1-3}$, we report average growth rate instead of growth rate at optimum temperature. The last two alternatives ($\mathcal{M}_{4-5}$) do not constrain cohort centers to a VBGF. We outline the fact that, although abundance and biomass can be computed with all alternatives, growth parameters and consequently production can only be computed with alternatives $\mathcal{M}_{1-3}$. Alternative $\mathcal{M}_5$ is the adaptation to our case study of the model presented by Ruiz and Laplanche (2010): cohort centers and standard deviations are random parameters (see Tables 2 and 3 of the latter reference). Alternative ($\mathcal{M}_4$) is the adaptation to our case study of the model discussed by Ruiz and Laplanche (2010): cohort centers are random and standard deviations are proportional to centers ($\sigma_{o,k} = \nu\mu_{o,k}$ with $\nu \sim$Gamma(0.001,0.001)). Alternative $\mathcal{M}_4$ is actually in-between alternatives $\mathcal{M}_3$ and $\mathcal{M}_5$ with random centers while standard deviations are constrained with an approximate VBGF ($\nu \simeq \sigma_\infty / L_\infty$ by using Eq. (5) with $L_0 \ll \mu_{o,k}$ and $\sigma_0 \ll \sigma_\infty$). All five alternatives are simulated with $K = 3$ Gaussian components and a $\Delta_l = 10$ mm length class, see Ruiz and Laplanche (2010) for insights supporting such a choice. Alternatives $\mathcal{M}_{1-3}$ are of equal complexity, $\mathcal{M}_{1-3}$ are less complex than $\mathcal{M}_4$, which is less complex than $\mathcal{M}_5$.

3 Results

Estimates of time of emergence are 101, 106, 68, 91, 106, 95 Julian days from 2005 to 2010, respectively. Point and interval estimates of parameters related to temperature and weight are provided in Appendix A (Supporting Infomation). Model fit ($\overline{D}$) and VBGF point parameter estimates ($\bar{G}$, L_0, L_∞, σ_0, σ_∞) are reported (Table 4; burn-in: $5\,10^5$; thinning: 10^3). Alternatives $\mathcal{M}_{1-3}$ and $\mathcal{M}_5$ provide similar fit ($633.9 \leq \overline{D} \leq 634.3$) whereas fit of alternative $\mathcal{M}_4$ is slightly worse ($\overline{D} = 637.0$). Informal penalization with complexity suggests that $\mathcal{M}_5$ is to be rejected, $\mathcal{M}_4$ is significantly better than $\mathcal{M}_5$, $\mathcal{M}_{1-3}$ are equivalent to each other and significantly

Table 4 Growth model alternatives, fit ($\overline{D}$), and growth point parameter estimates.

	Model alternatives					VBGF parameter estimates					Invariant parameter estimates		
	$\sigma_{o,k}$	$\mu_{o,k}$	G_t	$t^{\text{em}}_{o,k}$	$\overline{D}$	$10^3\bar{G}$	L_0	L_∞	σ_0	σ_∞	$\bar{G}L_\infty$	σ_0/L_0	σ_∞/L_∞
$\mathcal{M}_1$	√	√	√	√	634.3	0.471	28	419	4.5	83	0.18	0.16	0.16
$\mathcal{M}_2$	√	√	√	–	634.1	0.394	25	486	6.1	92	0.18	0.25	0.25
$\mathcal{M}_3$	√	√	–	–	633.9	0.843	37	282	6.5	57	0.23	0.18	0.18
$\mathcal{M}_4$	√	–	–	–	637.0	n.a.	n.a.	n.a.	n.a.	n.a.	n.a.	n.a.	0.15
$\mathcal{M}_5$	–	–	–	–	634.3	n.a.	n.a.	n.a.	n.a.	n.a.	n.a.	n.a.	n.a.

Reported growth parameters are average growth rate ($\bar{G} = G_{\text{opt}} \sum_t X_t / T$), length at emergence ($L_0$), asymptotic length ($L_\infty$), and standard deviations (σ_0 and σ_∞). The product $\bar{G}L_\infty$ as well as the coefficients of variation σ_0/L_0 and $\nu \simeq \sigma_\infty/L_\infty$ are also provided. Units are per day for growth rate ($\overline{G}$) and millimeters for lengths (L_0, L_∞, σ_0, σ_∞). Model alternatives are defined whether cohort standard deviations $\sigma_{o,k}$ ($\mathcal{M}_{1-4}$) and centers $\mu_{o,k}$ ($\mathcal{M}_{1-3}$) are constrained with a VBGF and whether growth rate G_t ($\mathcal{M}_{1-2}$) and date of emergence $t^{\text{em}}_{o,k}$ ($\mathcal{M}_1$) are temperature-dependent.

better than $\mathcal{M}_4$. In other words, constraining cohort centers and/or standard deviations with a VBGF does not (or slightly) worsen model fit while it significantly decreases complexity. As a result, alternatives $\mathcal{M}_{1-3}$ constraining both cohort centers $\mu_{o,k}$ and standard deviations $\sigma_{o,k}$ with a VBGF are to be preferred. The improvement which is provided by modeling temperature-dependent time of emergence and growth rate is not significant, in favor of selecting alternative $\mathcal{M}_3$ for this case study. Nevertheless, in the aim of illustrating the modeling of temperature-dependent time of emergence and growth rate, following results are computed by using baseline ($\mathcal{M}_1$).

Raw VBGF point parameter estimates are variable across models. For that reason, we also provide estimates of the product $\bar{G}L_\infty$ as well as the coefficients of variation σ_0/L_0 and σ_∞/L_∞ (Table 4). We provide interval estimates of growth parameters by using alternative $\mathcal{M}_1$ (Table 5, Supporting Infomation). Interval estimates of $\bar{G}L_\infty$ and σ_∞/L_∞ are of lesser amplitude than interval estimates of $\bar{G}$, L_∞, and σ_∞, in favor of reporting the former parameter estimates instead of raw VBGF parameters. This issue is discussed later.

Point and interval estimates of abundance ($\lambda_{o,k}$, λ_o, λ_k, λ), biomass ($B_{o,k}$, B_o), and production ($P_{o,k}$, P_o) variables are provided with `HMSPop` software. Some illustrations are provided and commented below, however. The multimodal decomposition of length-abundance plots is illustrated in Fig. 3 by plotting Eq. (1) with point estimates of parameters related to abundance ($\mu_{o,k}$, $\sigma_{o,k}$, $\tau_{o,k}$, and λ_o). Our model provides satisfactory results on this aspect. The VBGF by using temperature-dependent time of emergence and growth rate is illustrated in Fig. 4. Cohort dispersion, that is to say an increase of cohort standard deviation $\sigma_{o,k}$ with time, cohort overlapping, as well as seasonal variability of the growth rate (low in winter, highest in summer) are prominent in Fig. 4. We highlight the close relationship between Figs. 3 and 4: the three-component distributions of the eight subplots of Fig. 3 are snapshots at the eight campaign times of the three cohorts which growth is simulated in Fig. 4. We compare (Fig. 6, Supporting Infomation) three sets of cohort centers: centers $\bar{\mu}_{o,k}$ which are predicted by the VBGF ($\mathcal{M}_1$), centers $\mu_{o,k}$ used in the multimodal decomposition of length-abundance plots when assisted with the VBGF ($\mathcal{M}_1$), and centers $\mu_{o,k}$ computed by the abundance model alone ($\mathcal{M}_4$). The results show that three sets are of similar

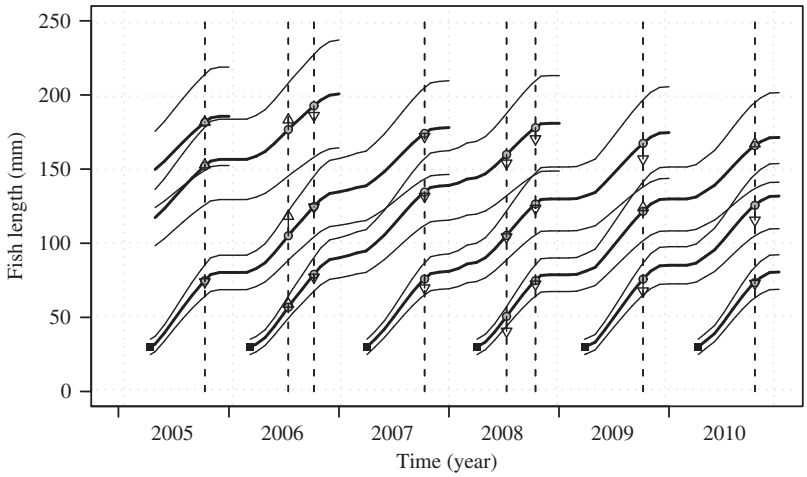

Figure 4 Cohort growth curves. Expected cohort centers (thick solid lines) plus and minus (thin solid lines) cohort standard deviations are computed by using the cohort growth model with the point estimates of the growth parameters which are reported in Table 5. Cohort centers at campaigns ($\bar{\mu}_{o,k}$ and $\mu_{o,k}$) are represented (circles and triangles, respectively). Squares: emergence (at time $t^{\mathrm{em}}_{o,k}$ of length L_o). Observation times t_o are highlighted with vertical dashed lines.

values. Estimates of production over biomass ratios ($(P/B)_{o,k}$ and $(P/B)_o$) are illustrated (Fig. 7, Supporting Infomation). $(P/B)_o$ values range between 1.03 and 1.59 per year.

4 Discussion

The results show that constraining cohort centers and standard deviations with a growth model is a fruitful approach in the aim of interpreting length-abundance plots. As a corollary, the modeling of individual fish growth with a VBGF as well as the statistical model of Appendix B (Supporting Infomation) are decisive steps toward a refined interpretation of length-abundance plots. Our feeling is that advanced modeling has the potential to enhance the value of removal sampling data by leading to estimates of parameters with ecological meaning (e.g. growth rate). HBMs have proven an efficient tool to fulfill this objective. Some choices have been made while constructing and simulating our HBM, which are discussed below. We also suggest some possible refinements and extensions to the current HBM.

Model selection has shown that the improvement brought by modeling temperature-dependent time of emergence and growth rate is not significant in this case study. The reasons are (i) stability of temperature across years resulting in stability of time of emergence $t^{\text{em}}_{o,k}$ and averaged growth rate $\bar{G}_{o,k}$ and (ii) sampling occurring mostly around the same date resulting in stability of the length of the time period between emergence and campaign $(t_o - t^{\text{em}}_{o,k})$, consequently resulting in stability of the cumulative growth rate $\bar{G}_{o,k}(t_o - t^{\text{em}}_{o,k})$. The consideration of removal sampling campaigns more scattered across the year, or of a study area with more variable temperatures, or of a longer study period, for instance in the aim of investigating the consequences of climate change on brown trout growth and production, would require the inclusion of temperature-dependent time of emergence and growth rate.

HBM framework would make it technically possible to handle missing water temperature data, simulate raw water temperatures (θ^w_t) for the whole duration of the study, and use such temperatures to compute temperature-dependent growth parameters. We, however, chose to compute temperature-dependent parameters by using predictions of water temperature ($\mathrm{E}[\theta^w_t]$) instead of raw values (θ^w_t). We provide three reasons supporting this choice. First, the use of predictions of water temperature instead of raw measurements leads to negligible consequences on computed time of emergence and growth rate, as discussed later. Second, the computations of time of emergence and growth rate (sums in Eqs. 3 and 7) during the MCMC simulation are time-consuming. The latter sums can be precomputed by using predictions of water temperature instead of raw values. Third, our aim is to provide a layout to compute growth parameter estimates of brown trout populations that could apply to previously acquired removal sampling data. The motivation for that is to investigate consequences of climate change, for instance over the last decades. Air temperature is available posterior to electrofishing campaigns by simply making a query to meteorological databases. Water temperature is more difficult to acquire and, in our case study, such measurements are only used to calibrate the air–water temperature submodel.

The joint simulation of the overall model was not feasible with the computation resources at hand. For that reason, we have simulated the overall model into three steps. The sequence of computations which is described below is illustrated in Fig. 1. The first step was to estimate the parameters of the weight and temperature submodels. Point parameter estimates of the latter submodels are used to predict fish weight (from fish length) and water temperature (from air temperature). At the second step, predictions of water temperature are used to compute time of emergence and growth rate. At the third step, the remaining submodels (abundance, growth, biomass, production) are simulated as a full HBM. We outline the fact that precomputation isolates submodels from the consecutive fully Bayesian inference. We see two consequences of that. First, presimulated submodels (e.g. emergence) cannot borrow information from other submodels (e.g. growth) to provide an improved estimation of parameters (e.g. CE_{50}). An extended discussion

on this issue is provided later. Second, uncertainty of parameters of precomputed submodels (e.g. η_o) is not propagated to parent submodels (e.g. biomass). Potential consequences would be an underestimation of the variance of the estimate of parameters of interest (e.g. $B_{o,k}$). A solution to the latter issue could be not to convey input values as fixed (as we have done here) but rather as random. In our case, however, the consequences of using fixed input values are negligible. The reason for that is that fish weights are summed to compute biomass, functions of water temperature are summed to compute time of emergence (Eq. 7) and growth rate (Eq. 3). See Ruiz and Laplanche (2010) for a demonstration regarding the consequences of using predictions of fish weight (instead of raw values with residual error) to compute biomass.

Estimates of growth parameters $\bar{G}$, L_∞, and σ_∞ are highly uncertain (Table 5, Supporting Infomation). The reason for that is that sports fishing takes place in the Neste d'Oueil from March to September with a 180 mm minimum size limit. Large, and consequently old, brown trouts are rare. The VBGF is approximately linear of slope $\bar{G}L_\infty$ for young fish, it is not feasible to jointly provide accurate estimates of $\bar{G}$ and L_∞ by using our data set. It is not either feasible to jointly provide accurate estimates of L_∞ and σ_∞ (Eq. 5 approximates to $\sigma_{o,k} \simeq (\sigma_\infty/L_\infty)\mu_{o,k}$ as shown earlier). We suggest three options. The first option, which we have chosen here, is to report more robust parameters such as $\bar{G}L_\infty$ and σ_∞/L_∞. The product $\bar{G}L_\infty$ is a life-history invariant which has already been reported in the literature (Mangel, 1996; Hutchings, 2002). The second option would be to provide multimodel estimates (Burnham and Anderson, 2002). The third option would be to use a distinct data set, e.g. collected in a fishing preserve, to provide estimates of $\bar{G}$, L_∞, and σ_∞. Estimation of length at emergence L_0 is relatively less uncertain. L_0 estimate is contingent on precalculated time of emergence, which is a function of temperature and time of oviposition. Time of emergence actually depends on more covariates, e.g. discharge (Capra et al., 2003). Time of oviposition has been roughly (in the absence of more appreciable information) assumed equal for all years. Oviposition timing is not punctual and depends on covariates. As a result, our estimates of L_0 should be considered with caution. An over (under) estimation of oviposition timing leads to an over (under) estimation of L_0. An inaccurate estimation of oviposition timing has, however, negligible consequences on other parameters (since L_0 is adjusted accordingly). Estimation of σ_0, and as a result σ_0/L_0, are uncertain. The posterior distribution of σ_0 (or quantiles, Table 5, Supporting Infomation) suggests to reduce of our growth model with $\sigma_0 = 0$. As a conclusion, we suggest to give credential to parameters $\bar{G}L_\infty$ and σ_∞/L_∞ and consider remaining parameters with caution.

HBM framework would make it technically possible to handle cardinal temperatures ($\theta_{\min}$, $\theta_{\max}$, θ_{opt}, θ_0, θ_1) as well as date of oviposition and critical value EC_{50} as random. The motivation for that would be to propagate the uncertainty of our knowledge on such parameters to estimates of remaining parameters. We have nevertheless considered cardinal temperatures, date of oviposition, and EC_{50} as constant. The main reason is that removal sampling data does not contains enough information to enhance our knowledge on the above parameters plus L_0 and G_{opt}. Randomizing cardinal temperatures, date of oviposition, and EC_{50} would result in randomizing time of emergence and cardinal growth rate. It is not possible, however, due to under-identification, to provide relevant estimates of time of emergence together with length at emergence (both represent variability of emergence) neither provide relevant estimates of cardinal growth rate together with optimum growth rate (both represent variability of growth rate). We chose to set constant time of emergence and cardinal growth rate (by setting constant cardinal temperatures, date of oviposition, and EC_{50}) in order to provide estimates of L_0 and G_{opt}. The interest of setting constant the former parameters is also to be able to carry out the (necessary) precomputations of time of emergence and cardinal growth rate.

Residuals $\bar{\mu}_{o,k} - \mu_{o,k}$ are low ($\sigma_\mu = 0.7$ (0.5, 1.3) mm) but are not negligible (Fig. 4). Residuals would be negligible if the reduction of the current model with the constraint of null residuals provided satisfactory results. Such a reduction did not provide satisfactory results (not shown) and we suggest several possible countermeasures. We have linearly interpolated monthly and 10-day air

temperatures to a daily time step. The use of daily air temperature measurements would be a first improvement. A more complex modeling of stream temperature, e.g. as a function of minimum and maximum daily air temperature and stream discharge, is a second option. A more complex modeling of the growth rate, e.g. as a function of discharge (Daufresne and Ranault, 2006), is a third option. The use of a more advanced statistical model of growth parameters, e.g. by correlating growth rate to asymptotic length or by adding an autoregressive component to the growth rate, is a possibility. At last, the use of a different growth function is also conceivable.

The model at the current state applies to riverine brown trout (*S. trutta fario*). Main model assumptions are that (i) reproduction occurs once a year, (ii) growth and emergence are predominantly dependent on water temperature, and (iii) temperature history at the stream section is a relevant indicator of temperature to which captured fish have been subjected to. Additional developments would be required to apply the model to species with a migrating behavior (e.g. brown trout morphs *S. trutta trutta* and *lacustris*) or with a different reproduction pattern. *S. trutta fario* also migrates, but operates low amplitude movements in order to switch for microhabitats. We highlight the fact that, for not to disturbing such natural movements as well as for practical reasons, we did not physically delimited the stream section across campaigns. Microhabitat movements are of limited consequences on temperature to which fish are subjected to. Temporal variations of abundance, however, are to be interpreted with caution: abundance (λ_o) is not synonymous with population size. Abundance is not representative of the size of a closed brown trout population inhabiting a stream section (such a population is fictional). Abundance rather depicts the status of a single species at a single place, which temporal variations are the result of some complex population dynamics. Finally, the stream section is not either physically delimited across removals. Results are potential entries and exits of fish during electrofishing, e.g. downstream exits of stunned but not caught fish. Consequences of the latter movements are an overestimate of electrofishing efficiency and an underestimate of abundance. A solution to this issue would be to position nets down- and up-stream while electrofishing.

To conclude, we highlight some possible extensions to the current model. First, the growth model could be perfected, as suggested above. Date of oviposition could be modeled and related to covariates. Removal sampling data could be accompanied with age data in the aim of facilitating cohort decomposition. To achieve this goal, age of fish could be evaluated through scalimetry (age is determined by counting growth zones of fish scales magnified with a microscope) on a sample of caught fish and treated as missing data on the rest. The model could be extended with an additional spatial structure in order to deal with multiple sampling sections (Wyatt, 2002; Ebersole et al., 2009; Ruiz and Laplanche, 2010). Parameters (e.g. growth parameters) could be spatially related to each other or related to spatially distributed environmental covariates (Wyatt, 2003; Webster et al., 2008). Parameters of the multimodal description of length-abundance plots are cohort centers, standard deviations, and weights ($\tau_{o,k}$) as well as total abundance (λ_o). We have constrained centers and standard deviations with a growth model. Weights and abundance could also be constrained with a population dynamics submodel. Parameters of the population dynamics submodel could be spatially related to each other or to covariates. The motivation is to build a single framework which would provide interval estimates of a large panel of descriptors indicative of brown trout populations at a large spatio-temporal scale. Such a model could be used to evaluate, compare, and predict the status of brown trout populations, e.g. consequently to climate change.

Acknowledgements The authors are indebted to L. Pacaux, F. Dauba, and P. Lim (Ecolab) for their contribution in conducting the electrofishing campaign and collecting the removal sampling data set. The authors are grateful to EDF R&D for financing the electrofishing campaign and providing the water temperature data set. The authors thank both anonymous referees for their valuable, detailed reviews which significantly improved the clarity of the manuscript. This work was granted access to the HPC resources of CALMIP under the allocation 2011-P1113

Conflict of interest

The authors have declared no conflict of interest.

References

Armstrong, J., Kemp, P., Kennedy, G., Ladle, M. and Milner, N. (2003). Habitat requirements of atlantic salmon and brown trout in rivers and streams. *Fisheries Research* **62**, 143–170.

Bertalanffy, L. (1938). A quantitative theory of organic growth (inquiries on growth laws II). *Human Biology* **10**, 181–213.

Burnham, K. and Anderson, D. (2002). *Model Selection and Multimodel Inference: A Practical Information-Theoretic Approach*. 2nd edn., Springer, Berlin.

Caissie, D. (2006). The thermal regime of rivers: a review. *Freshwater Biology* **51**, 1389–1406.

Capra, H., Sabaton, C., Gouraud, V., Souchon, Y. and Lim, P. (2003). A population dynamics model and habitat simulation as a tool to predict brown trout demography in natural and bypassed stream reaches. *River Research and Applications* **19**, 551–568.

Carle, F. and Strub, M. (1978). A new method for estimating population size from removal data. *Biometrics* **34**, 621–630.

Chen, Y., Jackson, D. and Harvey, H. (1992). A comparison of von Bertalanffy and polynomial functions in modelling fish growth data. *Canadian Journal of Fisheries and Aquatic Sciences* **49**, 1128–1235.

Congdon, P. (2006). *Bayesian Statistical Modelling*. *Wiley Series in Probability and Statistics*. 2nd edn.Wiley, Chichester, England.

Crawley, M. (2007). *The R Book*. Wiley, New York.

Daufresne, M. and Renault, O. (2006). Population fluctuations, regulation and limitation in stream-living brown trout. *Oikos* **113**, 459–468.

Dorazio, R., Jelks, H. and Jordan, F. (2005). Improving removal-based estimates of abundance by sampling a population of spatially distinct subpopulations. *Biometrics* **61**, 1093–1101.

Ebersole, J., Colvin, M., Wigington, P., Leibowitz, S., Baker, J., Church, M., Compton, J. and Cairns, M. (2009). Hierarchical modeling of late-summer weight and summer abundance of juvenile Coho Salmon across a stream network. *Transactions of the American Fisheries Society* **138**, 1138–1156.

Elliott, J. (1994). *Quantitative Ecology and the Brown Trout*. Oxford University Press, Oxford, UK.

Elliott, J. and Hurley, M. (1998). An individual-based model for predicting the emergence period of sea trout fry in a lake district stream. *Journal of Fish Biology* **53**, 414–433.

Elliott, J., Hurley, M. and Fryer, R. (1995). A new, improved growth model for brown trout, Salmo trutta. *Functional Ecology* **9**, 290–298.

Fontoura, N. and Agostinho, A. (1996). Growth with seasonally varying temperatures – an expansion of the von Bertalanffy growth model. *Journal of Fish Biology* **48**, 569–584.

Froese, R. and Pauly, D. (2010). Fishbase. World Wide Web electronic publication. `www.fishbase.org`

Gelman, A., Carlin, J., Stern, H. and Rubin, D. (2003). *Bayesian Data Analysis*. Chapman & Hall/CRC, Boca Raton, Florida.

Gelman, A. and Rubin, D. (1992). Inference from iterative simulation using multiple sequences. *Statistical Science* **7**, 457–472.

Gouraud, V., Baglinière, J., Baran, P., Sabaton, C., Lim, P. and Ombredane, D. (2001). Factors regulating brown trout populations in two french rivers: application of a dynamic population model. *Regulated Rivers: Research & Management* **17**, 557–569.

Hutchings, J. (2002). Life histories of fish. In: *Handbook of Fish Biology and Fisheries*. Vol. 1, Blackwell Science Ltd, Malden, USA, pp. 149–174.

Jensen, A. and Johnsen, B. (1999). The functional relationship between peak spring floods and survival and growth of juvenile Atlantic salmon (*Salmo salar*) and brown trout (*Salmo trutta*). *Functional Ecology* **13**, 778–785.

Jonsson, B. and Jonsson, N. (2009). A review of the likely effects of climate change on anadromous atlantic salmon *Salmo salar* and brown trout *Salmo trutta*, with particular reference to water temperature and flow. *Journal of Fisheries Biology*, **75**, 2381–2447.

Klemetsen, A., Amundsen, P.-A., Dempson, J., Jonsson, B., Jonsson, N., OConnell, M. and Mortensen, E. (2003). Atlantic salmon *Salmo salar* l., brown trout *Salmo trutta* l. and arctic charr *Salvelinus alpinus* (l.): a review of aspects of their life histories. *Ecology of Freshwater Fish* **12**, 1–59.

Kwak, J. and Waters, T. (1997). Trout production dynamics and water quality in Minnesota streams. *Transactions of the American Fisheries Society* **126**, 35–48.

Lagadic, L., Caquet, T., Amiard, J.-C. and Ramade, F. (1998). *Utilisation de biomarqueurs pour la surveillance de la qualité de l'environnement*. Lavoisier TEC DOC, Paris.

Laplanche, C. (2010). A hierarchical model to estimate fish abundance in alpine streams by using removal sampling data from multiple locations. *Biometrical Journal*, **52**, 209–221.

Lobón-Cerviá, J. (1991). *Dinámica de poblaciones de peces en ríos: pesca eléctrica y métodos de capturas sucesivas en la estima de abundancias*. Monografías del Museo Nacional de Ciencias Naturales, Madrid.

Lunn, D., Spiegelhalter, D., Thomas, A. and Best, N. (2009). The BUGS project: Evolution, critique and future directions. *Statistics in Medicine* **28**, 3049–3067.

Mallet, J., Charles, S., Persat, H. and Auger, P. (1999). Growth modelling in accordance with daily water temperature in European grayling (*Thymallus thymallus* L.). *Canadian Journal of Fisheries and Aquatic Sciences* **56**, 994–1000.

Mangel, M. (1996). Life history invariants, age at maturity and the ferox trout. *Evolutionary Ecology*, **10**, 249–263.

Mäntyniemi, S., Romakkaniemi, A. and Arjas, E. (2005). Bayesian removal estimation of a population size under unequal catchability. *Canadian Journal of Fisheries and Aquatic Sciences* **62**, 291–300.

Mohseni, O., Stefan, H. and Erickson, T. (1998). A nonlinear regression model for weekly stream temperatures. *Water Resource Research* **34**, 2685–2692.

Morrill, J., Bales, R. and Conklin, M. (2005). Estimating stream temperature from air temperature: implications for future water quality. *Journal of Environmental Engineering* **131**, 139–146.

Nash, J. and Sutcliffe, J. (1970). River flow forecasting through conceptional models, 1. a discussion of principles. *Journal of Hydrology* **10**, 282–290.

Nordwall, F., Näslund, I. and Degerman, E. (2001). Intercohort competition effects on survival, movement, and growth of brown trout (*Salmo trutta*) in Swedish streams. *Canadian Journal of Fisheries and Aquatic Sciences* **58**, 2298–2308.

Ntzoufras, I. (2009). *Bayesian Modeling Using WinBUGS*. Wiley, Hoboken, NJ.

Pauly, D. and Moreau, J. (1997). *Méthodes pour l'évaluation des ressources halieutiques*. Cépaduès-Editions, Toulouse, France.

Peterson, J., Thurow, R. and Guzevich, J. (2004). An evaluation of multipass electrofishing for estimating the abundance of stream-dwelling salmonids. *Transactions of the American Fisheries Society* **133**, 462–475.

Pinheiro, J. and Bates, D. (2000). *Mixed-Effects Models in S and S-Plus*. Springer, Berlin.

Pitcher, T. (2002). A bumpy old road: Sized-based methods in fisheries assessment. In: *Handbook of Fish Biology and Fisheries*, Vol. 2, Blackwell Science Ltd., Malden, USA, pp. 189–210.

Polard, T., Jean, S., Gauthier, L., Laplanche, C., Merlina, G., Sanchez-Perez, J.-M. and Pinelli, E. (2011). Mutagenic impact on fish of runoff events in agricultural areas in south-west france. *Aquatic Toxicology* **101**, 126–134.

Quinn, T. and Deriso, R. (1999). *Quantitative Fish Dynamics*. Oxford University Press, USA.

Riley, S. and Fausch, K. (1992). Underestimation of trout population size by maximum likelihood removal estimates in small streams. *North American Journal of Fisheries Management* **12**, 768–776.

Rivot, E., Prevost, E., Cuzol, A., Baglinière, J.-L. and Parent, E. (2008). Hierarchical Bayesian modelling with habitat and time covariates for estimating riverine fish population size by successive removal method. *Canadian Journal of Fisheries and Aquatic Science* **65**, 117–133.

Robert, C. and Casella, G. (2004). *Monte Carlo Statistical Methods*. 2nd edn., Springer, New York.

Rosso, L., Lobry, J., Bajard, S. and Flandrois, J. (1995). Convenient model to describe the combined effects of temperature and ph on microbial growth. *American Society for Microbiology* **61**, 610.

Ruiz, P. and Laplanche, C. (2010). A hierarchical model to estimate the abundance and biomass of salmonids by using removal sampling and biometric data from multiple locations. *Canadian Journal of Fisheries and Aquatic Science* **67**, 2032–2044.

Shinn, C. (2010). Impact of toxicants on stream fish biological traits. PhD thesis, Université de Toulouse.
Somers, I. (1988). On a seasonally-oscillating growth function. *Fishbyte* **6**, 8–11.
Spiegelhalter, D., Best, N., Carlin, B. and van der Linde, A. (2002). Bayesian measures of model complexity and fit. *Journal of the Royal Statistical Society Series B* **64**, 583–639.
Taylor, C. (1960). Temperature, growth, and mortality – the pacific cockle. *ICES Journal of Marine Science* **26**, 117.
Ward, R. (2002). Genetics of fish populations. In: *Handbook of Fish Biology and Fisheries*, **vol. 1**, Blackwell Science Ltd., Malden, USA, pp. 200–224.
Webb, J. and McLay, H. (1996). Variation in the time of spawning of Atlantic salmon (*Salmo salar*) and its relationship to temperature in the Aberdeenshire Dee, Scotland. *Canadian Journal of Fisheries and Aquatic Science* **53**, 2739–2744.
Webster, R. A., Pollock, K. H., Ghosh, S. K. and Hankin, D. G. (2008). Bayesian spatial modeling of data from unit-count surveys of fish in streams. *Transactions of the American Fisheries Society* **137**, 438–453.
Wood, C. (2007). Global warming: implications for freshwater & marine fish. In: *Society for Experimental Biology Seminar Series*, Vol. 61, Cambridge University Press, Cambridge.
Wyatt, R. (2002). Estimating riverine fish population size from single- and multiple-pass removal sampling using a hierarchical model. *Canadian Journal of Fisheries and Aquatic Science* **59**, 695–706.
Wyatt, R. (2003). Mapping the abundance of riverine fish populations: integrating hierarchical Bayesian models with a geographic information system (GIS). *Canadian Journal of Fisheries and Aquatic Science* **60**, 997–1006.